Separation Science and Technology
Publication details, including instructions for authors and subscription information:
http://www.informaworld.com/smpp/title~content=t713708471

Estimation of Mass Transfer Rates through Hydrophobic Pervaporation Membranes

Amy R. Overington[a]; Marie Wong[a]; John A. Harrison[b]; Lílian B. Ferreira[c]
[a] Institute of Food, Nutrition, and Human Health, Massey University, Auckland, New Zealand [b] Institute of Fundamental Sciences, Massey University, Auckland, New Zealand [c] Fonterra Co-operative Group Ltd., Palmerston North, New Zealand

To cite this Article Overington, Amy R. , Wong, Marie , Harrison, John A. and Ferreira, Lílian B.(2009) 'Estimation of Mass Transfer Rates through Hydrophobic Pervaporation Membranes', Separation Science and Technology, 44: 4, 787 — 816
To link to this Article: DOI: 10.1080/01496390802697106
URL: http://dx.doi.org/10.1080/01496390802697106

Separation Science and Technology, 44: 787–816, 2009

ISSN: 0149-6395 print/1520-5754 online
DOI: 10.1080/01496390802697106

Taylor & Francis
Taylor & Francis Group

Estimation of Mass Transfer Rates through Hydrophobic Pervaporation Membranes

Amy R. Overington,[1] Marie Wong,[1] John A. Harrison,[2] and Lílian B. Ferreira[3]

[1]Institute of Food, Nutrition, and Human Health, Massey University, Auckland, New Zealand
[2]Institute of Fundamental Sciences, Massey University, Auckland, New Zealand
[3]Fonterra Co-operative Group Ltd., Palmerston North, New Zealand

Abstract: In pervaporation of dilute solutions (acids, esters, and ketones) through hydrophobic membranes, mass transfer coefficients increased with temperature in an Arrhenius-like manner. Activation energies and pre-exponential factors were estimated through empirical correlations, allowing estimation of mass transfer coefficients. The activation energy was a function of the heat of sorption and the elastic modulus of the membrane. For low molecular weight compounds, the heat of sorption was the more important of these two factors, whereas the membrane thickness (which influenced the elastic modulus) became more important for larger compounds. The compensation effect allowed pre-exponential factors to be estimated from the activation energies.

Keywords: Activation energy, compensation effect, heat of sorption, pervaporation, pre-exponential factor

Received 31 July 2008; accepted 26 November 2008.
Address correspondence to Amy R. Overington, Fonterra Co-operative Group, Ltd., Private Bag 11029, Palmerston North, New Zealand. Tel.: +64-6-350-4600 extn. 64951; Fax: +64-6-356-1476. E-mail: Amy.Overington@fonterra.com

INTRODUCTION

Pervaporation is a separation process in which the composition of a mixed liquid feed is altered by selective permeation through a non-porous membrane. The permeate is in the vapor state, because the permeate side is kept under vacuum (1,2). Pervaporation is a promising technology for the recovery of organic compounds from dilute aqueous solutions, using hydrophobic membranes. Applications include concentrating flavor compounds and recovering solvents from waste streams (3–5). Pervaporation has several advantages over alternative organic compound recovery techniques: no additives are necessary, energy usage is not high, the product remains natural (in the case of flavour recovery), and low to moderate operating temperatures mean that thermal degradation either does not occur or is minimized (4,6,7).

Many researchers have presented models for mass transfer through pervaporation membranes, with most based on the solution-diffusion model (2,5). However, overall mass transfer rates (from the bulk feed, through the membrane, to the permeate collection vessel) can vary depending on the membrane structure, membrane module and process used (2), making it difficult to compare results obtained by different researchers. Hence, it is hard to predict pervaporation performance without at least some experimental data on the pervaporation system in question.

The objective of this study was to develop empirical correlations, relating the properties of selected flavor compounds (organic acids, esters, and ketones) to their pervaporation fluxes under various operating conditions (membrane type, feed temperature, and permeate pressure).

THEORY

For steady-state transport processes, fluxes are proportional to the driving force (8), with the proportionality constant defined as the mass transfer coefficient (9):

$$J_i = k_i \times \textit{driving force} \tag{1}$$

where J_i is the flux of component i and k_i is the overall mass transfer coefficient of component i.

Driving Force

In the absence of an electrical potential driving force, all common driving forces in membrane processes can be reduced to a gradient in chemical potential across the membrane (8,10). The solution-diffusion model,

which is the most commonly used model to describe pervaporation, assumes that this chemical potential gradient is expressed as a concentration or activity gradient (rather than a total pressure gradient as in the pore flow model) (10). Several expressions for the pervaporation driving force are used in the literature, with the most common being partial pressure difference (11–13), activity difference (14,15) and concentration difference (16) between the feed and permeate sides of the membrane. Partial pressure and activity driving forces are closely related, with partial pressure being the product of activity and saturated vapor pressure (17). The mass transfer coefficient with a partial pressure driving force may be divided by the saturated vapor pressure, in order to express the mass transfer coefficient in terms of an activity driving force (18).

Concentration difference as a driving force does not take into account any non-ideal effects, and therefore is a poor approximation of the true driving force, because aqueous solutions containing organic compounds of low solubility frequently show non-ideal behaviour (19,20). Hence, Pereira et al. (20) concluded that a chemical potential driving force (based on logarithmic activity difference) led to more accurate results than an approximation based on concentration difference.

In this study, the driving force was approximated by the activity difference between the upstream and downstream sides of the membrane. Activities on the feed and permeate sides were estimated from Eqs. (2) and (3) respectively (12,18):

$$a_{i,f} = x_{i,f}\gamma_{i,f} \tag{2}$$

$$a_{i,p} = \frac{p_{i,p}}{p_i^0(T_f)} \tag{3}$$

where $a_{i,f}$ and $a_{i,p}$ are the activities of compound i in the feed and permeate respectively, $x_{i,f}$ is the mole fraction of compound i in the feed, $\gamma_{i,f}$ is the activity coefficient of compound i, $p_{i,p}$ is the partial pressure of compound i on the permeate side and $p_i^0(T_f)$ is the saturated vapour pressure of compound i at the feed temperature.

The flux was thus given by the following expression, based on Trifunović et al. (21):

$$J_i = k_i\left(\gamma_i x_{i,f} - \frac{P_{i,p}}{p_i^0}\right) \tag{4}$$

Mass Transfer Coefficients

The mass transfer coefficient includes mass transfer through all steps in the pervaporation process: mass transfer through the feed boundary

layer, through the membrane and out into the permeate side (22). This can be described using a resistance-in-series model (8,16,22):

$$\frac{1}{k_i} = \frac{1}{k_{i,bl}} + \frac{1}{k_{i,m}} + \frac{1}{k_{i,p}} \tag{5}$$

In Eq. (5), $k_{i,bl}$ is the mass transfer coefficient of compound i through the feed boundary layer, $k_{i,m}$ is the mass transfer coefficient through the membrane and $k_{i,p}$ is the mass transfer coefficient on the permeate side. All of these mass transfer coefficients depend on the pervaporation system, the operating conditions, and the permeant compound.

Pervaporation fluxes generally increase as the temperature is raised. The effect of temperature may be described by an Arrhenius-type relationship. When Arrhenius activation energies for pervaporation are reported in the literature, they are normally calculated from the slope of a plot of $\ln(J)$ versus $1/T$. To distinguish the effect of temperature on permeability from its effect on the driving force, Feng and Huang (23) recommended plotting ln(*permeability*), instead of $\ln(J)$, to calculate the activation energy for permeation. The current study followed Feng and Huang's recommendation, except that overall mass transfer coefficients (defined as $J/\Delta a$) were used instead of membrane-thickness-normalized permeability (defined by Feng and Huang (23) as $J/\Delta p$). Therefore, the following equation related the mass transfer coefficient to the temperature:

$$\ln(k_i) = \ln(k_0) - \frac{E_a}{RT} \tag{6}$$

where k_0 is the pre-exponential factor, E_a is the activation energy of permeation, and R is the gas constant. From Eq. 6, the mass transfer coefficient is a function of the pre-exponential factor and the activation energy. The activation energy is itself a function of several parameters, which are outlined in Fig. 1 and discussed in the following paragraphs.

It is well known that the diffusion of small molecules in polymers is an activated process (24–26), being described by an Arrhenius-type equation as long as the temperature range is not too large. The activation energy for molecular diffusion through a polymer corresponds to the energy required for permeant molecules to jump from one free volume hole to the next free volume hole in the polymer (27,28). This means that the activation energy required for diffusion should increase with molecular size (27). However, in pervaporation, other parameters besides diffusion influence the rate of movement through the membrane, and thus the dependence of the total activation energy on molecular size is more complex.

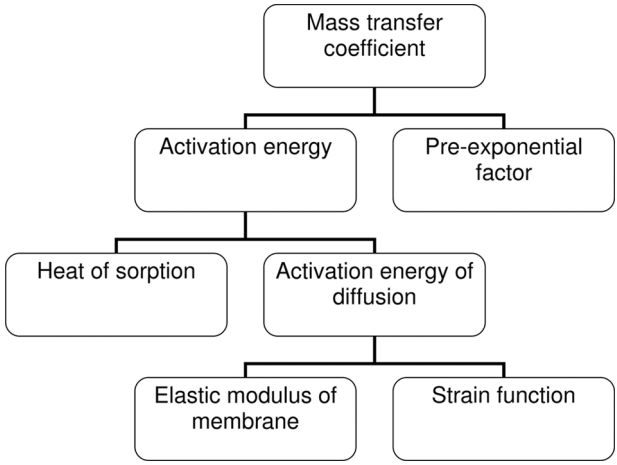

Figure 1. Hierarchy of important parameters in the mass transfer correlation.

The apparent activation energy for permeation is a combination of the energy required for sorption and the energy required for diffusion (23,27):

$$E_a = \Delta H_s + E_D \tag{7}$$

where E_a is the apparent activation energy of permeation, ΔH_s is the molar heat of sorption, and E_D is the activation energy of diffusion.

Barrer (24) calculated that the activation energy for diffusion through a lattice is a function of the displacement of molecules making up the lattice (i.e. the strain), and depends on whether the lattice is elastic or rigid. Pönitsch and Kirchheim (29) (following a derivation by Zener (30)) applied this theory to diffusion in polymers, using the elastic modulus as a measure of elasticity, to create the equation:

$$E_D = M_0 f(\varepsilon) \tag{8}$$

where M_0 is the elastic modulus extrapolated to a reference temperature (taken in this study to be -121°C, the glass transition temperature of PDMS (50)) and $f(\varepsilon)$ is a function of the average strain encountered as the permeant moves from site to site within the polymer. According to (29), the principle applies equally to rubbery and glassy polymers, as long as the strain does not relax during the time period in which a permeant jumps between sites in the polymer. Substituting Eq. (8) into Eq. (7) gives the following equation:

$$E_a = \Delta H_s + f(\varepsilon) M_0 \tag{9}$$

Thus, referring again to Fig. 1, the mass transfer coefficient may be modelled as a function of four parameters: the heat of sorption, the membrane's elastic modulus, the strain function, and the pre-exponential factor.

In some Arrhenius-type relationships, the activation energy and the pre-exponential factor are not independent. A linear relationship has been observed between the logarithm of the pre-exponential factor and the activation energy (or between the entropy change and the enthalpy change) for many different chemical processes (31), including diffusion in polymers (25,32–34) and sorption in foods (35) and solvents (36). This relationship is generally referred to as the compensation effect. According to the transition state theory, the logarithm of the pre-exponential factor is proportional to the activation entropy in a process, and the activation energy is related to the enthalpy difference between the activated and normal states (25). Accordingly, compensation between entropy and enthalpy will lead to a relationship between the activation energy and the pre-exponential factor. However, in the case of diffusion, the pre-exponential factor also depends on the length of each activated jump within the polymer (25), meaning that the compensation effect in this situation is not fully explained by entropy–enthalpy compensation.

Although there has been some debate over whether the compensation effect is real or a mathematical artifact (31,37), Pönitsch and Kirchheim (29) (following a derivation by Zener (30)) proposed a physical reason for the compensation effect for diffusion in polymers, relating both the activation energy and the pre-exponential factor to the elastic modulus of the polymer.

In cases where the compensation effect applies, the pre-exponential factor may be estimated as a function of the activation energy. Therefore, predicted values for the mass transfer coefficient and hence the flux could be calculated for different compounds and different operating conditions.

EXPERIMENTAL MASS TRANSFER COEFFICIENTS

Experimental fluxes were taken from a previous study (38), in which the pervaporation fluxes of nine flavor compounds (acids, esters and ketones), and the total flux, were measured at feed temperatures between 20°C and 40°C, a feed flow rate of $1\,L\,min^{-1}$, and permeate pressures ranging from 0.3 kPa to 3.3 kPa. The membrane active layers consisted of polydimethylsiloxane (PDMS Type 1, ~0.5 μm thickness; PDMS Type 2, ~1.5 μm thickness) or polyoctylmethylsiloxane (POMS, 5–6 μm thickness; a value of 5.5 μm was used in calculations). Membranes were supplied by GKSS-Forschungszentrum Geesthacht GmbH (Geesthacht,

Germany). The feed was a dilute multicomponent solution, consisting of the flavor compounds listed in Table 1, dissolved in distilled water. The feed composition did not significantly change during each four-hour pervaporation experiment. The total fluxes with this model solution were negligibly different from the water flux (38). The concentration of each flavor compound in the permeate was determined using gas chromatography (38); the individual compound fluxes were calculated from the permeate concentrations and the measured total flux. Full experimental details are given in (38); all of the fluxes measured during that study were used to develop the correlations in the present work.

The driving force for permeation was calculated from Eq. (4). Saturated vapor pressures of water, esters, and ketones were taken from the literature (39–41) and were interpolated over the temperature range of interest (20–40°C). Vapor pressures of acids were estimated using the Wagner equation (Eq. (10)), using constants tabulated in Poling et al. (42).

$$\ln p_i^0 = \ln p_c + \left(\frac{T_c}{T}\right)(a\tau + b\tau^{1.5} + c\tau^{2.5} + d\tau^5) \tag{10}$$

In Eq. (10), p_c is the critical pressure, T is the feed temperature, T_c is the critical temperature, a, b, c and d are empirical constants and τ is given by the equation:

$$\tau = 1 - \frac{T}{T_c} \tag{11}$$

Table 1. Composition of the model feed solution used for all experiments[a]

Compound	Molecular weight ($g\,mol^{-1}$)	Feed concentration ($mg\,L^{-1}$)
Acids		
Acetic acid	60	105
Butanoic acid	88	107
Hexanoic acid	116	111
Octanoic acid	144	105
Esters		
Ethyl butanoate	116	101
Ethyl hexanoate	144	100
Ethyl octanoate	172	10.4
Ketones		
2-Heptanone	114	9.8
2-Nonanone	142	9.8

[a]All flavor compounds were supplied by Sigma-Aldrich Co. (St Louis, MO, USA), and had purities of greater than 98%.

The activity coefficients of the flavor compounds were assumed to be equal to those at infinite dilution, as the feed solution was very dilute (no compound had a concentration greater than 111 ppm). This is a common assumption for pervaporation with dilute aqueous feeds (13,43,44). The dilute feed also meant that the activity coefficient of water could be assumed to be unity (45). Infinite dilution activity coefficients of acids and ketones were calculated using correlations and constants listed in Poling et al. (42). For ethyl butanoate, experimentally determined activity coefficients were taken from Carelli et al. (46). Activity coefficients at each required temperature were interpolated from these literature data, except for ethyl hexanoate and ethyl octanoate, because constants to calculate the activity coefficients of these compounds were given only at 20°C in Poling et al. (42). However, as Carelli et al. (46) showed that the activity coefficient for ethyl butanoate varied by only 10% over the temperature range 25–65°C, the 20°C values from Poling et al. (42) were assumed to give a satisfactory estimate for the activity coefficients of ethyl hexanoate and ethyl octanoate between 20 and 40°C. Poling et al. (42) stated that the variation of the activity coefficient with the temperature is usually much smaller than the variation of saturated vapor pressure, and therefore it is acceptable to disregard the temperature dependence of the activity coefficient in calculations of this type. This assumption was also applied to pervaporation by Olsson and Trägårdh (45).

Once the driving force was calculated in this way for each compound, the overall mass transfer coefficient could be determined for each compound with each membrane and each temperature (Eq. (4)). Mass transfer coefficients do not usually vary with permeate pressure (12); hence, the mass transfer coefficient was taken as the mean for all runs at a particular temperature.

RESULTS AND DISCUSSION

Fluxes of Different Compounds

Figure 2 gives the concentration-normalized fluxes of each compound (38), at a feed temperature of 30°C and a permeate pressure of 2 kPa as an example. These fluxes have been normalized by dividing by the feed concentration, to enable compounds at different concentrations to be compared. In dilute feed solutions, fluxes are generally directly proportional to the feed concentration (3,19); this was also confirmed using the feed solution for the current study at half the original concentration (data not shown). Esters and ketones had similar concentration-normalized fluxes, which were greater than those of acids. Within esters

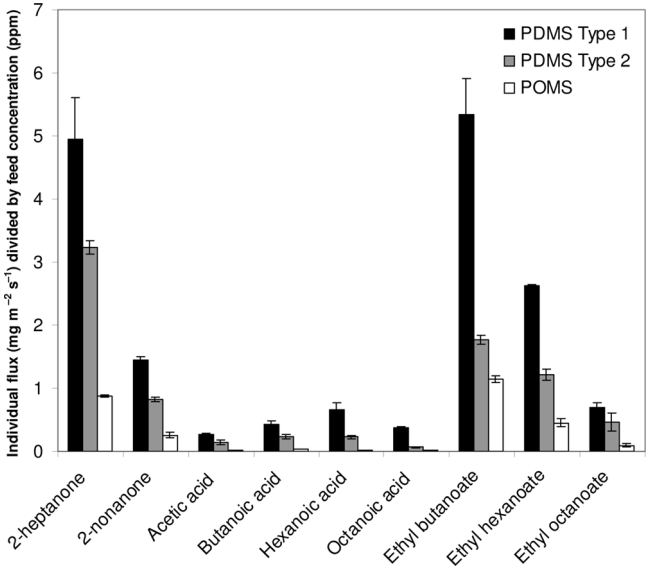

Figure 2. Concentration-normalized fluxes (mean ± standard error of at least three replicates) of model solution compounds, at 30°C and 2 kPa, with three different membranes.

and ketones, the concentration-normalized fluxes decreased with an increase in molecular weight, but, within acids, this trend applied only to acids with molecular weights greater than 88–116 g mol^{-1} (depending on the membrane and the operating conditions); smaller acids showed the opposite trend. Some reasons for these trends were discussed in a previous paper (38).

Effect of Temperature on Mass Transfer

Fluxes increased with temperature by about one order of magnitude, on average, between 20 and 40°C (38). This agrees with a well-known trend, and is due to an increased membrane permeability at raised temperatures, as well as an increase in feed activity creating a higher driving force (3,4,23). Changes in the driving force due to temperature can be estimated by examining literature data for the saturated vapour pressures of permeants over the temperature range of interest, and using Eq. (4). However, the mass transfer coefficient is more difficult to predict for different systems, as it depends on both the permeant and the membrane (47).

Both the driving force and the permeability contribute to the increase in flux with temperature, but the relative importance of these two factors can vary. Olsson and Trägårdh (45) found that the increase in water flux with increasing temperature (through a POMS membrane) was largely due to the increased driving force; however, for aroma compounds, they found that increased permeability at higher temperatures influenced flux enhancement to a similar or greater degree than driving force. Similar results were found in the current study: the driving force of water increased more than threefold from 20 to 40°C, but the driving forces of other compounds increased only slightly (data not shown).

The mass transfer coefficients increased with temperature according to an Arrhenius-type relationship (Eq. 6). Figure 3 shows this relationship for each compound, with the PDMS Type 1 membrane. Within each class of compound, the mass transfer coefficients decreased with increasing molecular weight. The PDMS Type 2 membrane also gave linear Arrhenius plots (not shown). Only two temperatures were tested with the POMS membrane, but it was assumed that the POMS membrane would also follow an Arrhenius-type relationship, based on the results with the PDMS membranes, as well as from the work of other authors with various membranes including POMS (16,23,45). Therefore, activation energies and pre-exponential factors were calculated for POMS based on this assumption. Activation energies related to molecular weight are shown in Fig. 4.

Effect of Compound and Membrane Type on Activation Energy

The activation energy of permeation is a combined parameter, which is dependent on several factors relating to both the permeant and the membrane (Eq. 9). This is shown by Fig. 4, in which the activation energies showed different behavior with increasing size within each homologous series, depending on the membrane used.

The membrane type had a significant effect on the activation energy of some compounds, but not others. The activation energies of small permeants (with molecular weights lower than about 120 g mol^{-1}), especially esters and ketones, were not influenced by the type of membrane. In contrast, the activation energies of larger compounds varied widely between the three membranes tested, with compounds needing the greatest activation energy to pass through the PDMS Type 1 membrane, followed by the PDMS Type 2 membrane and then the POMS membrane. This corresponded to PDMS Type 1 having the highest fluxes, followed by PDMS Type 2 and then POMS, indicating that membranes with higher fluxes had a greater temperature dependence.

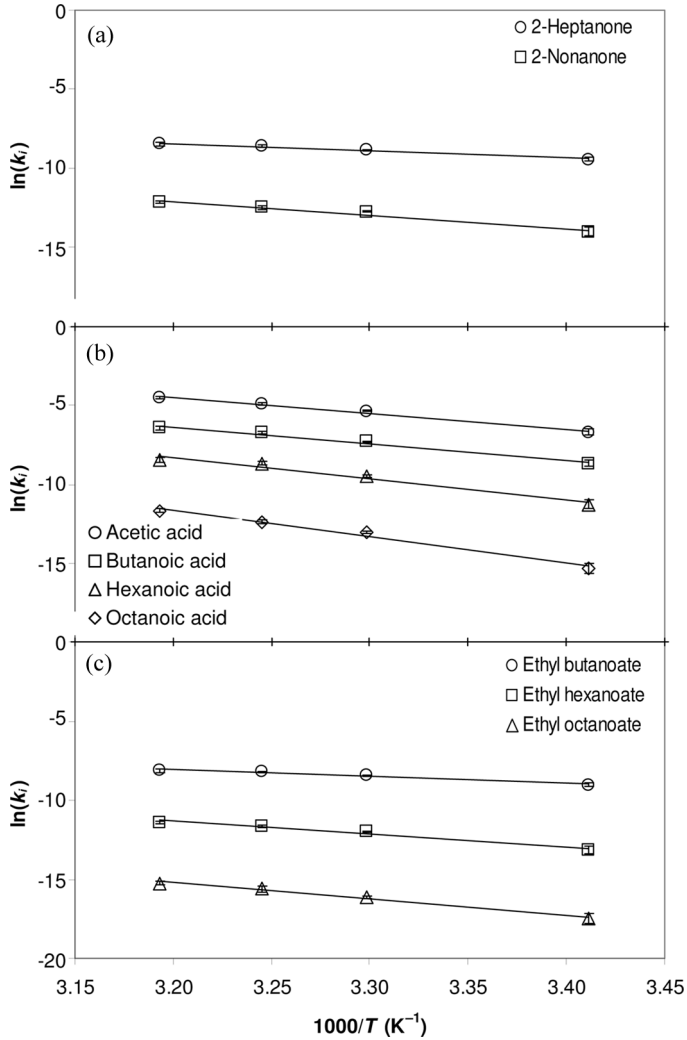

Figure 3. Arrhenius plots of (a) ketone, (b) acid and (c) ester mass transfer coefficients (PDMS Type 1 membrane). Data points are mean ± standard error of 3–17 measurements at each temperature.

This distinction between small and large permeants was also observed by Dole et al. (48), who analysed their own and literature data on the activation energies for diffusion of various compounds in several packaging polymers. They suggested that polymer mobility may be important for the diffusion of large molecules only, whereas, for small

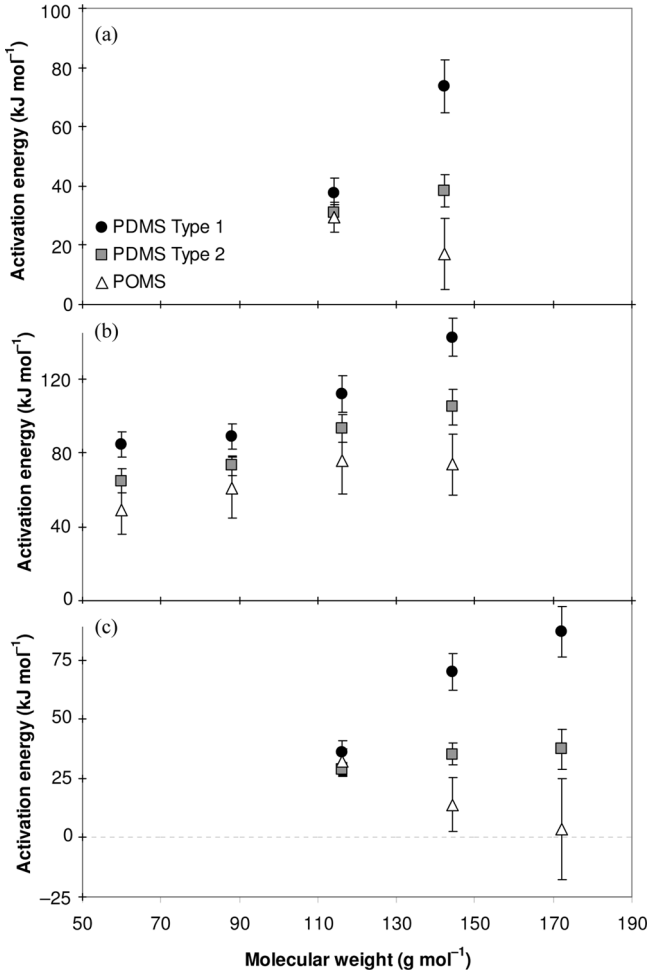

Figure 4. Relationships between activation energy for permeation (mean ± standard error) and molecular weight, for (a) ketones, (b) acids and (c) esters. Activation energies calculated from Arrhenius plots with 27–35 data points.

molecules, the intrinsic mobility of the permeant is more important regardless of polymer type.

Tikhomirov et al. (49) discussed the differences in activation energy of diffusion above and below the glass transition temperature of the polymer. In general, diffusion below the glass transition temperature involves the permeant moving between pre-existing holes, whereas, at higher temperatures, it normally also involves creating larger holes as a

result of polymer chain movement. Which of these two mechanisms is rate limiting above the glass transition temperature depends on the permeant size as well as the polymer type (49). In the current study, all experiments were carried out well above the glass transition temperature of −121°C for PDMS (50) (no glass transition data were available for POMS, but it is a similar polymer to PDMS), and the change at approximately 120 g mol^{-1} in Fig. 4 fits with the theory that there is a change in the rate-limiting factor for permeants above a certain molecular size.

Below 120 g mol^{-1}, the activation energy increased with increasing molecular weight within the acids (this trend could not be confirmed for the other functional groups, because only one ester and one ketone below this critical size were tested). Kabra et al. (51) found that the activation energy for pervaporation was greater for butanoic acid than for propanoic acid, which fits with the trends in Fig. 4. As the permeant size increases, its diffusivity in the membrane decreases. Consequently, as the permeants move through the membrane, it is less likely that larger permeating molecules will find a free volume hole in the polymer of appropriate size into which to jump, and therefore the activation energy should increase with molecular size, consistent with the trend for small acids in Fig. 4.

In an apparent contradiction, the fluxes of small acids (acetic acid, butanoic acid, and usually hexanoic acid, depending on the operating conditions) increased with molecular weight (Fig. 2), even though, as the activation energy increases (that is, as permeation becomes more difficult), the flux would be expected to decrease. One reason for this is that flux depends on both the mass transfer coefficient and the driving force. As the molecular weight increased within each class of compound, the overall mass transfer coefficient decreased but the activity difference across the membrane increased, leading to the flux either increasing or decreasing, depending on whether the mass transfer coefficient or the driving force was the dominant factor. Liang and Ruckenstein (52) found that membranes for which the flux was lower had a higher activation energy. However, their activation energy was calculated based on the flux rather than the mass transfer coefficient. This means that it represented the effect of temperature on both the mass transfer coefficient and the driving force together, rather than considering them separately as in the current study.

Ketones and esters had similar activation energies for the same molecular weight, whereas the activation energies of acids were considerably higher. This was reflected in the relative fluxes of each class of compound; after normalizing for different feed concentrations, ketones and esters had fluxes several times higher than those of acids. As the elastic moduli of PDMS films have been found to increase with decreasing film

thickness (53), it therefore follows that thinner membranes should require greater activation energies (Eq. (9)). This was indeed found to be the case for compounds with molecular weights greater than 120 g mol^{-1} (Fig. 4). Shishatskii et al. (54) also showed that the density of polymer films increased as their thickness decreased, meaning that the cohesive energy density, and hence the activation energy for diffusion, was greater with thinner membranes (54).

Estimated M_0 values for the PDMS Type 1, PDMS Type 2, and POMS membranes were 102, 34, and 10 MPa, respectively. M_0 for PDMS was estimated by taking values for the elastic modulus of the bulk polymer at a range of temperatures (55), and then accounting for the membrane thickness by extrapolating Wang et al.'s (53) elasticity data for various film thicknesses (at their lowest measured strain of 5%). No literature data were available for the elastic modulus of POMS, but it was estimated to be about 2.2 times that of PDMS (in the bulk polymer), using a group contribution method explained by van Krevelen (27). Assuming that the elastic moduli of both POMS and PDMS were influenced by membrane thickness in the same way, Wang et al.'s PDMS data (53) were again extrapolated to estimate the elastic modulus of POMS at the membrane thickness used.

Figure 5, which shows Eq. (9) graphically, has y-intercepts equal to ΔH_S (assuming that this is similar for both PDMS and POMS) and slopes depending on $f(\varepsilon)$. Therefore, this figure can be used to distinguish between the two components of the apparent activation energy: the heat of sorption and the activation energy of diffusion. The slopes of the best fit lines in Fig. 5 are large and positive for compounds with molecular weights greater than 120 g mol^{-1}, and closer to zero for compounds below this critical molecular weight (especially water, 2-heptanone and ethyl butanoate). This means that, for small compounds, the total activation energy is almost entirely determined by the heat of sorption, with the activation energy of diffusion having very little influence. In contrast, the activation energy for larger compounds is strongly influenced by the energy required to diffuse through the polymer matrix.

The intercepts of Fig. 5 are given in Fig. 6, which shows two distinct groups. In the acids (including water) homologous series, ΔH_S increased with molecular weight, except for octanoic acid. In the esters and ketones series, ΔH_S was lower than that for acids, and decreased linearly with molecular weight. The heat of sorption is a combination of the energy required to make a void in the polymer and the energy given off when that void is filled by a permeant molecule (56). As larger compounds would require a larger void, the former quantity would increase with molecular weight. However, as larger compounds of the functional groups tested here are also more hydrophobic, they would be expected

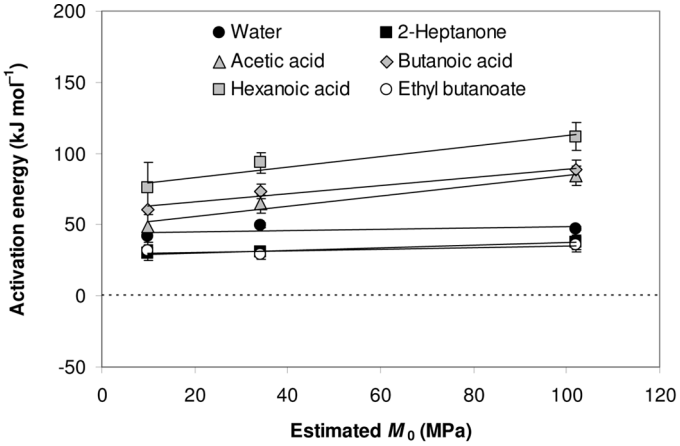

(a)

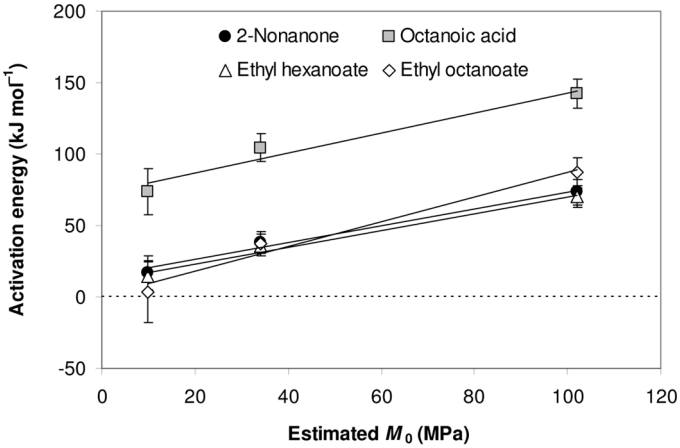

(b)

Figure 5. Activation energy versus estimated elastic modulus: (a) compounds with molecular weights less than 120 g mol^{-1}; (b) compounds with molecular weights greater than 120 g mol^{-1}.

to release more energy when associating with the hydrophobic polymers making up these membranes. Figure 6 seems to indicate that of these two factors, the hydrophobicity effect is more important for esters and ketones, but the molecular size effect is more important for acids (except for octanoic acid).

Literature data regarding the heats of sorption of flavor compounds in the polymers studied here are scarce, so the ΔH_S values in Fig. 6 could

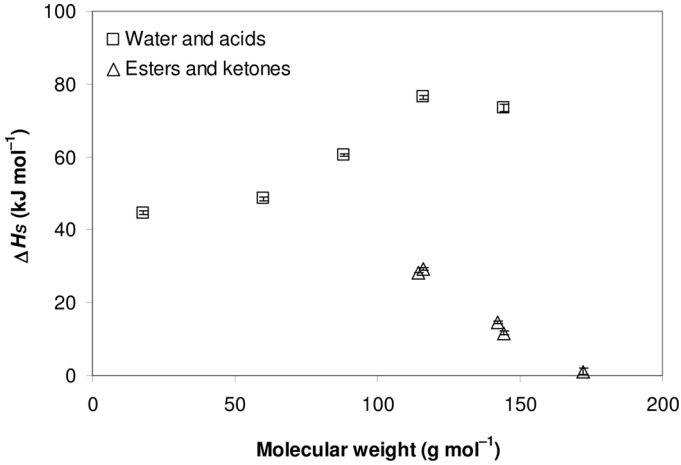

Figure 6. Heat of sorption (mean ± standard error of the intercept of Figure 5) versus molecular weight, for water, acids, esters and ketones.

only be verified for those compounds for which sorption coefficients were available in the literature at more than one temperature (ethyl butanoate and ethyl hexanoate). For these two compounds, ΔH_S could be estimated from the Arrhenius-type equation (27):

$$S = S_0 \exp\left(\frac{-\Delta H_s}{RT}\right) \tag{12}$$

in which S is the sorption coefficient and S_0 is the pre-exponential factor for sorption. Table 2 shows that the heats of sorption in Fig. 6 have the same order of magnitude as those calculated from independent data. Their similarity increases confidence in the data in Fig. 6 and Eq. (9). However, Eq. (12) must be used with some caution in this case because sorption coefficients at only two temperatures, with slightly different polymers, were used in the calculation. The heat of sorption of water in non-polar polymers has been reported to be around $25\,\mathrm{kJ\,mol^{-1}}$ (27), somewhat lower than the value from Fig. 6.

Olsson and Trägårdh (45) suggested that it could be possible to predict activation energies from each permeant's functional group, its activity coefficient at infinite dilution in water (which influences hydrophobicity and therefore solubility in the membrane) and its liquid molar volume (which influences diffusivity in the membrane). Figures 5 and 6 support their hypothesis that the activation energy is influenced by the functional group and the molecular size (evaluated as molecular weight

Table 2. Heats of sorption calculated from literature data (Eq. (12)) and from Fig. 6

	Sorption coefficient			Heat of sorption ($kJ\,mol^{-1}$)	
Compound	18°C in POMS (58)	20°C in POMS (calculated from (59))	25°C in silicone rubber (57)	Eq. (12)	Figure 6 (mean ± standard error)
Ethyl butanoate		21.4	29.3	45.7	29.1 ± 0.3
Ethyl hexanoate	241.3		264.6	9.5	11.6 ± 0.5

in the current study), but also show that the membrane thickness is an important factor affecting the activation energies of certain compounds. Djebbar et al. (60) found no obvious relationship between activation energy and compound or membrane type, but their apparent activation energies were determined based on the increase in flux with temperature, rather than the increase in mass transfer coefficient with temperature as recommended by Feng and Huang (23).

Relationship between Activation Energy and Pre-Exponential Factor

The logarithms of the pre-exponential factors normalized for membrane thickness ($k_0 \times l$) varied with compound and membrane in a similar pattern to the activation energies, suggesting that the compensation effect applied to the studied pervaporation system. Figure 7 shows the compensation effect between $\ln(k_0 \times l)$ and E_a/R, for which the slopes were similar for all compounds but the intercepts varied between different compounds. The average slope of this graph was $0.0031\,K^{-1}$ (standard error of $\pm 0.0001\,K^{-1}$). When the slope of each compound's line was fixed to this average value, the intercepts varied depending on the molecular weight, as shown by Fig. 8. The following empirical relationship gave a good fit for the data in Fig. 8 ($R^2 = 0.998$):

$$\ln(-y_{\text{intercept}}) = 4.00 \times 10^{-5} M^{1.87} + 2.80 \qquad (13)$$

where $y_{\text{intercept}}$ is the y-intercept of Fig. 7 ($\ln(k_0 \times l)$ when $E_a/R = 0$) and M is molecular weight.

van Krevelen (27) postulated the following relationship between the activation energy and the pre-exponential factor for permeation in

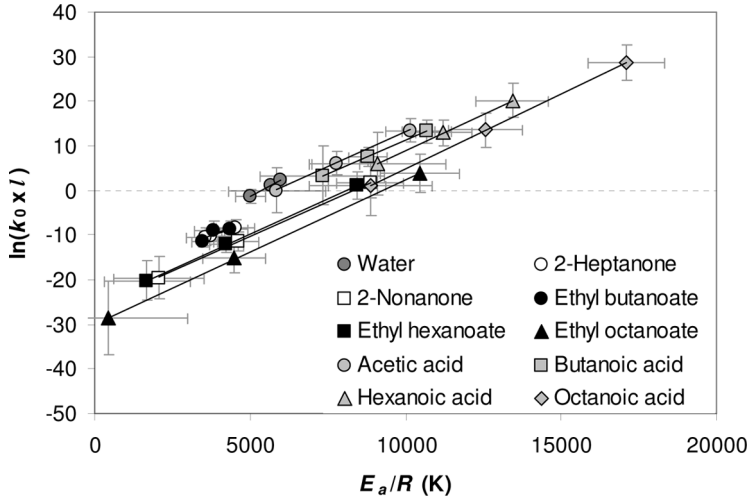

Figure 7. Compensation effect between activation energy and pre-exponential factor. Error bars show standard errors of the slope and intercept of Arrhenius plots.

rubbery polymers (converted to natural logarithm units instead of $\log_{10}$ as given by van Krevelen (27)):

$$\ln(k_0) = 0.0023\frac{E_a}{R} - 23.2 \tag{14}$$

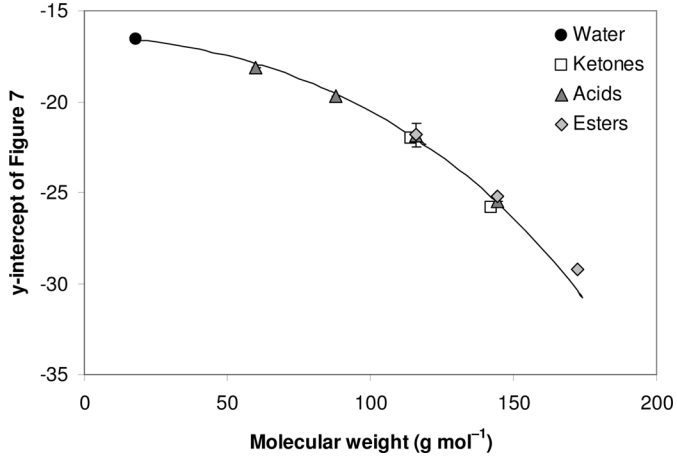

Figure 8. Variation of compensation effect between compounds (mean ± standard error of the y-intercept of Fig. 7; three data points per compound).

The constants in Eq. (14) are slightly different from those determined in this study (in Fig. 7, the slope of each line was close to $0.0031\ K^{-1}$ and the intercepts ranged from -29.8 to -18.3). The difference may be because van Krevelen's equation refers to the permeation of gases through polymers (27), as opposed to the current study which focuses on pervaporation of flavour compounds.

In this study, the slope of Fig. 7 was close to the inverse of the average operating temperature. Kirchheim and Huang (61) explained how, in the case of diffusion, this result arises mathematically from the form of the compensation equation rather than for any physical reason, provided that the difference in diffusivity between matrices (different membranes in this case) is small compared with the difference in activation energies. They argued that, although the compensation effect works mathematically in this case, it could not be used to explain the physical diffusion mechanism when applied to an individual permeant diffusing in different matrices (as opposed to different permeants diffusing in the same matrix).

However, there is more of a physical basis to explain why the compensation effect for sorption, rather than diffusion, depends on temperature. Liu and Guo (31) summarized a theory relating the compensation effect to entropy and enthalpy changes occurring when a solute dissolves in a solvent. This is relevant to pervaporation, because sorption into the membrane is one of the contributing factors to the permeability. According to the theory (31), when a species X dissolves in a solvent A, two processes occur at once: the nominal process, in which X is transferred from its own environment into the solvent environment $X\backslash a$; and the environmental process, in which some A molecules, which were surrounded by other A molecules in the environment $A\backslash a$, are transferred into the environment of the solute $A\backslash x$. The environmental process may involve enthalpy and entropy changes, but the free energy change for the environmental process is zero (31). This means that the enthalpy change (ΔH) and the entropy change (ΔS) must offset each other, so that:

$$\Delta H - T\Delta S = 0$$
$$\frac{\Delta H}{\Delta S} = T \tag{15}$$

If the entropy and enthalpy changes for the environmental process are much larger than their counterparts for the nominal process, then the proportionality constant in the compensation effect equation will be approximately the inverse temperature (31), because ΔH is related to the activation energy and ΔS is related to the logarithm of the pre-exponential factor.

The compensation effect has not been reported before for pervaporation, but it has been observed for the permeabilities of gases in polymers (26,27). Permeability is a combination of two processes, sorption and diffusion. Budrugeac and Segal (62) discussed how, for a two-step process, an apparent compensation effect occurs if an apparent rate constant is used rather than each process being evaluated separately. This implies that the compensation effect observed in the current study is an apparent effect.

A false compensation effect occurs if there are experimental errors in the data such that the estimated values for k_0 and E_a are correlated, even though their true values are not (31). Correlation between the estimated values occurs because k_0 and E_a are not determined independently, so that any experimental errors in the data used to calculate them will translate into correlated errors in both k_0 and E_a. To establish whether an apparent compensation effect is real or false, Liu and Guo (31) recommended drawing error bars on the compensation plot. The standard errors on each point in Fig. 7 were relatively small compared with the variation between data points; hence, the overall linear relationship between $\ln(k_0 \times l)$ and E_a/R exists even when errors are taken into account. Therefore, in this case, the compensation effect is not likely to be caused by experimental error.

Independent of whether the compensation effect observed in the current study has a true physical origin, the observed correlation in Fig. 7 can be used practically to estimate the pre-exponential factor from the activation energy.

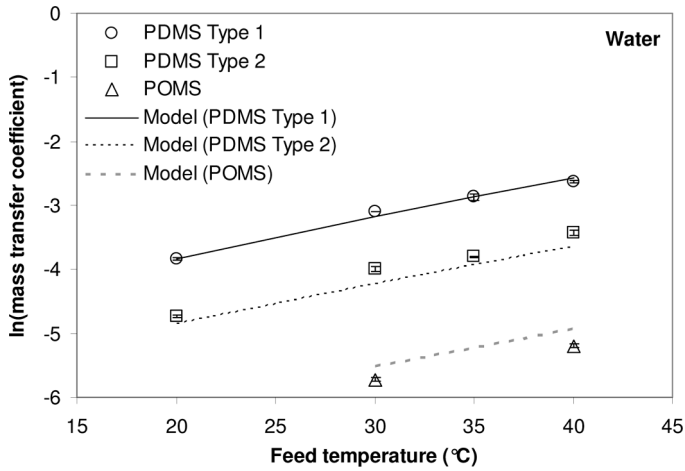

Figure 9. Mass transfer coefficients for water. Symbols are experimental values (mean ± standard error of at least three replicates) and lines show model predictions.

Estimation of Mass Transfer Coefficients using Correlations

Activation energies for each compound and each membrane were determined from Eq. (9), taking values of ΔH_S from Fig. 6 and using the slope of Fig. 5 as $f(\varepsilon)$. Each compound's molecular weight was substituted into Eq. (13), to obtain a value for the y-intercept of Fig. 7. The activation energy and the y-intercept were then used to

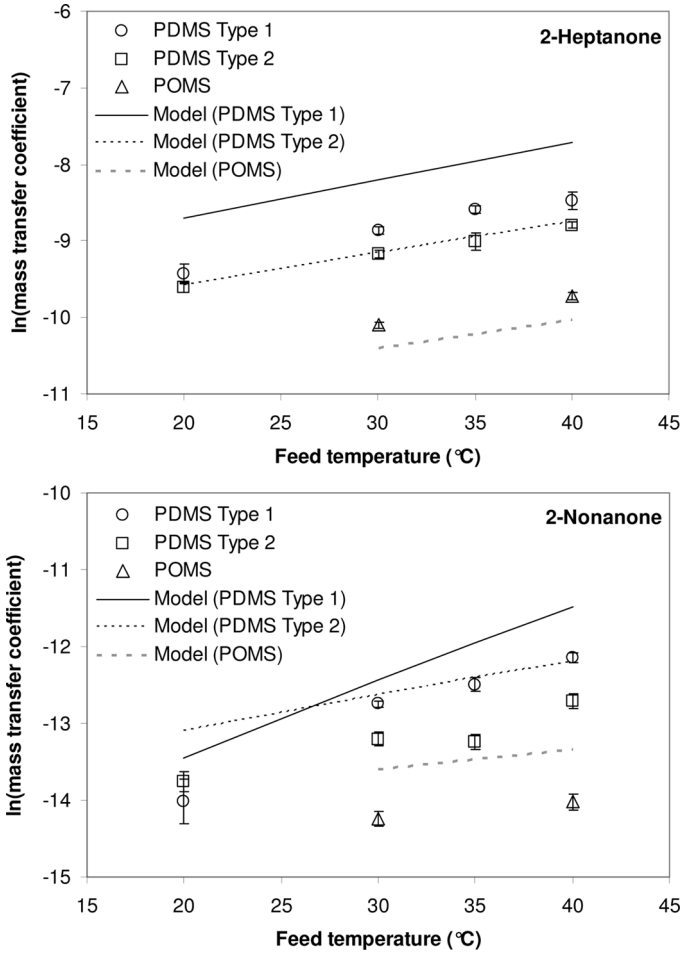

Figure 10. Mass transfer coefficients for ketones. Symbols are experimental values (mean ± standard error of at least three replicates) and lines show model predictions.

calculate the pre-exponential factor, using Eq. (16), in which 0.0031 was the average slope from Fig. 7.

$$\ln(k_0) = 0.0031\frac{E_a}{R} + y_{\text{intercept}} \tag{16}$$

Mass transfer coefficients at each temperature could then be estimated by substituting the calculated pre-exponential factors and activation energies into the Arrhenius equation. These estimated mass transfer coefficients are compared with experimental mass transfer coefficients in Fig. 9 (water), Fig. 10 (ketones), Fig. 11 (acids) and Fig. 12 (esters). These figures show that the accuracy of the curve fitting varied for different compounds. The activation energies were close to the experimental values, which meant that the slopes of the lines in Figs. 9–12 (that is, the influence of temperature on the mass transfer coefficient) were similar to the experimental data. However, estimated mass transfer coefficients were often above or below the experimental values by up to 1.5 logarithmic units. In general, the greatest deviations between the model and the experimental data occurred for the largest compounds moving through the stiffest polymer (PDMS Type 1). Complex permeant-polymer interactions, which are not accounted for in this simple mass

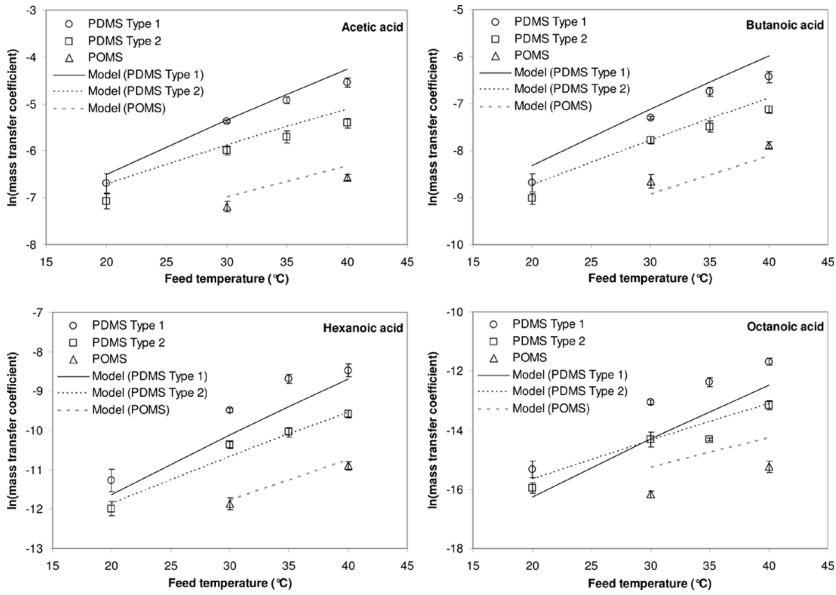

Figure 11. Mass transfer coefficients for acids. Symbols are experimental values (mean ± standard error of at least three replicates) and lines show model predictions.

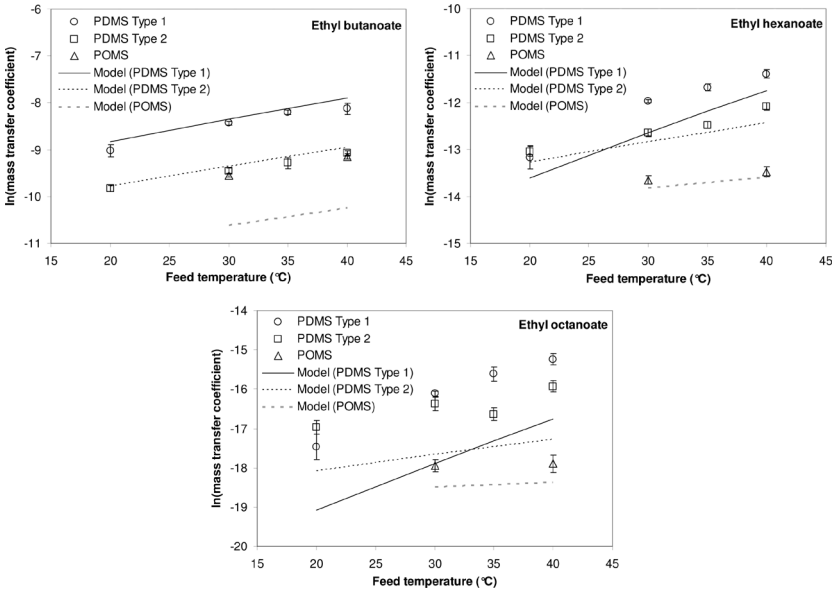

Figure 12. Mass transfer coefficients for esters. Symbols are experimental values (mean ± standard error of at least three replicates) and lines show model predictions.

transfer model, are more likely to occur in this situation than when smaller compounds move through more elastic polymers.

The best fits were obtained for those compounds that had correlation coefficients close to one in Fig. 7 and that lay on the best fit line in Fig. 8 (water, ethyl hexanoate, acetic acid, butanoic acid and hexanoic acid). Ethyl butanoate and 2-heptanone were the only compounds with R^2 less than 0.99 in Fig. 7; more membranes of different thicknesses would be needed to improve this.

The estimated mass transfer coefficients were then multiplied by the calculated activity driving force in order to estimate the fluxes. The estimated fluxes were compared with actual measured fluxes for the total flux and all the individual flavor compound fluxes (Fig. 13). Figure 13 shows that, although there was some scatter, the total and individual fluxes were well modelled overall, with R^2 values of 0.97 and 0.85 respectively. Therefore, this method could be used to gain an estimate of the flux for flavor compounds of the tested functional groups.

Although the model is empirical and hence applies only to this particular pervaporation system, it is expected that similar models could be developed for other pervaporation systems, by changing the empirical

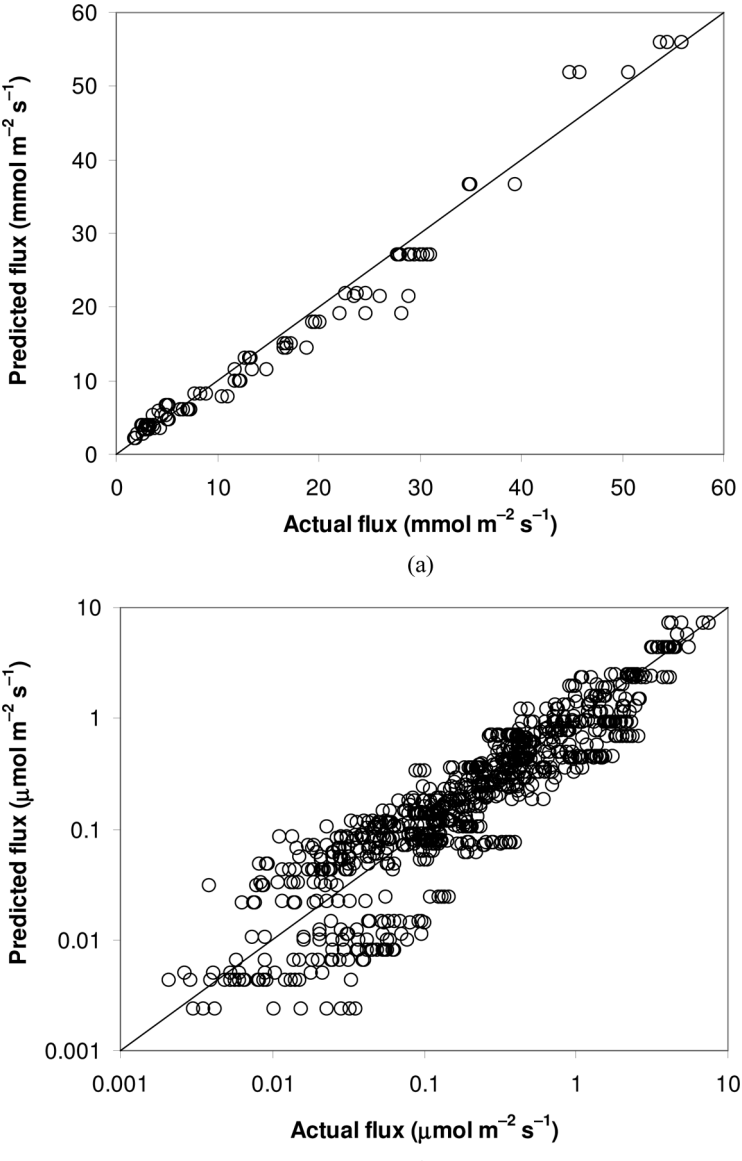

Figure 13. Predicted versus experimental fluxes of (a) water (total flux; $R^2 = 0.97$) and (b) flavor compounds ($R^2 = 0.85$). The diagonal line is an ideal 1:1 relationship between the two.

constants. Indeed, the model has recently been tested for its ability to estimate fluxes of compounds in two feed mixtures that were not used in model development (63). The first feed mixture contained the same flavor compounds as in the current work, plus 20% (w/v) dairy fat. The fat did not permeate through the membrane, but it altered the driving forces of permeants through its interaction with the flavor compounds. With this feed mixture, the measured fluxes of water and esters were close to the fluxes estimated using the model. However, the current model could not accurately estimate acid and ketone fluxes in the modified feed mixture. The fat would have altered the energy required for some compounds to move from the feed mixture into the membrane (i.e., the heat of sorption), which means that the model would need to be altered in order to work well with this modified feed mixture (63).

The second feed mixture was an aqueous solution of diacetyl and many minor flavour compounds. The model worked best at a feed temperature of 20°C, at which temperature the flux of diacetyl could be estimated to within 3% of its measured flux (63).

CONCLUSIONS

The apparent activation energy is a complex property in pervaporation, and it depends on both the permeant and the membrane. The differences in activation energy for various permeant/membrane combinations were explained by splitting the total activation energy into its constituent parts: the heat of sorption and the activation energy of diffusion. The activation energy of diffusion was an important contributor to the total apparent activation energy only for compounds larger than a certain critical size. For these compounds, thinner membranes had higher activation energies because of their greater elastic moduli. For smaller compounds, thermodynamic factors, such as the heat of sorption, were more important than the activation energy of diffusion.

As the activation energy for low molecular weight compounds was not highly dependent on the elastic modulus, this suggests that the membrane polymer chains did not need to stretch for these small compounds to permeate. It can be concluded that the free volume spaces in the membranes tested were large enough to accommodate these small compounds.

It was shown that the compensation effect, which has previously been observed for sorption and diffusion processes, also applied to this pervaporation system. Using this relationship, the pre-exponential factor could be calculated from the activation energy. Fluxes could therefore be empirically estimated for this pervaporation system, as a function of the elastic modulus of the membrane, experimental values of each

compound's heat of sorption and $f(\varepsilon)$, and the empirical relationship between the activation energy and the pre-exponential factor. The compensation effect provides a useful way of estimating mass transfer coefficients without needing to independently determine the pre-exponential factor.

The model is applicable to some, though not all, systems beyond the feed solution from which it was developed. The empirical constants may need to be altered for different pervaporation systems. The model would need to be tested with a wider range of compounds and membranes, in order to establish the physical meaning of the empirical constants.

ACKNOWLEDGEMENTS

This work was funded by Fonterra Co-operative Group Ltd and the Foundation for Research, Science and Technology, New Zealand (contract number FCGL0403). The membranes were kindly supplied by GKSS-Forschungszentrum.

NOMENCLATURE

a	Activity (dimensionless)
a,b,c,d	Empirical constants (Eq. (10))
E_a	Activation energy ($kJ\,mol^{-1}$)
E_D	Activation energy of diffusion ($kJ\,mol^{-1}$)
ΔH	Enthalpy change ($kJ\,mol^{-1}$)
ΔH_S	Heat of sorption ($kJ\,mol^{-1}$)
J	Flux ($mol\,m^{-2}\,s^{-1}$)
k	Mass transfer coefficient ($mol\,m^{-2}\,s^{-1}$)
k_0	Pre-exponential factor ($mol\ m^{-2}\ s^{-1}$)
l	Membrane thickness (m)
M	Molecular weight ($g\ mol^{-1}$)
M_0	Elastic modulus extrapolated to a reference temperature (Pa)
p	Partial pressure (Pa)
p_i^0	Vapour pressure of compound i in the pure state (Pa)
R	Gas constant ($8.314\,J\ mol^{-1}\ K^{-1}$)
S	Sorption coefficient (dimensionless)
S_0	Pre-exponential factor for sorption (dimensionless)
ΔS	Entropy change ($kJ\ mol^{-1}\ K^{-1}$)
T	Temperature (K)
x	Mole fraction (dimensionless)
$y_{intercept}$	y-Intercept of Fig. 7

Greek Letters

γ	Activity coefficient (dimensionless)
ε	Strain (dimensionless)
τ	Defined by Eq. (11) (dimensionless)

Subscripts

bl	In feed boundary layer
c	Critical
f	On feed side of membrane
i	Component *i* or membrane piece *i*
m	In membrane
p	On permeate side of membrane

REFERENCES

1. Néel, J. (1991) Introduction to Pervaporation. In: *Pervaporation Membrane Separation Processes*, Huang, R.Y.M. ed.; Elsevier Science Publishers: Amsterdam, The Netherlands, 1–110.
2. Lipnizki, F.; Trägårdh, G. (2001) Modelling of pervaporation: Models to analyze and predict the mass transport in pervaporation. *Sep. Purif. Methods*, *30* (1): 49–125.
3. Peng, M.; Vane, L.M.; Liu, S.X. (2003) Recent advances in VOCs removal from water by pervaporation. *J. Hazard. Mater.*, *98* (1–3): 69–90.
4. Lipnizki, F.; Hausmanns, S.; Ten, P.K.; Field, R.W.; Laufenberg, G. (1999) Organophilic pervaporation: Prospects and performance. *Chem. Eng. J.*, *73* (2): 113–129.
5. Karlsson, H.O.E.; Trägårdh, G. (1993) Pervaporation of dilute organic-waters mixtures. A literature review on modelling studies and applications to aroma compound recovery. *J. Membr. Sci.*, *76* (2–3): 121–146.
6. Willemsen, J.H.A.; Dijkink, B.H.; Togtema, A. (2004) Organophilic pervaporation for aroma isolation—industrial and commercial prospects. *Membrane Technology*, *2*: 5–10.
7. Karlsson, H.O.E.; Trägårdh, G. (1997) Aroma recovery during beverage processing. *J. Food Eng.*, *34* (2): 159–178.
8. Mulder, M. (1996) *Basic Principles of Membrane Technology*; Kluwer Academic Publishers: Dordrecht, The Netherlands.
9. Zydney, A.L. (1997) Stagnant film model for concentration polarization in membrane systems. *J. Membr. Sci.*, *130* (1–2): 275–281.
10. Wijmans, J.G.; Baker, R.W. (1995) The solution-diffusion model—a review. *J. Membr. Sci.*, *107* (1–2): 1–21.
11. Baker, R.W.; Wijmans, J.G.; Athayde, A.L.; Daniels, R.; Ly, J.H.; Le, M. (1997) The effect of concentration polarization on the separation of volatile organic compounds from water by pervaporation. *J. Membr. Sci.*, *137* (1–2): 159–172.
12. Baudot, A.; Souchon, I.; Marin, M. (1999) Total permeate pressure influence on the selectivity of the pervaporation of aroma compounds. *J. Membr. Sci.*, *158* (1–2): 167–185.

13. Trifunović, O.; Trägårdh, G. (2006) Mass transport of aliphatic alcohols and esters through hydrophobic pervaporation membranes. *Sep. Purif. Technol.*, *50* (1): 51–61.
14. Jiraratananon, R.; Chanachai, A.; Huang, R.Y.M. (2002) Pervaporation dehydration of ethanol-water mixtures with chitosan/hydroxyethylcellulose (CS/HEC) composite membranes II. Analysis of mass transport. *J. Membr. Sci.*, *199* (1–2): 211–222.
15. Lipnizki, F.; Hausmanns, S.; Field, R.W. (2004) Influence of impermeable components on the permeation of aqueous 1-propanol mixtures in hydrophobic pervaporation. *J. Membr. Sci.*, *228* (2): 129–138.
16. Karlsson, H.O.E.; Loureiro, S.; Trägårdh, G. (1995) Aroma compound recovery with pervaporation—temperature effects during pervaporation of a muscat wine. *J. Food Eng.*, *26* (2): 177–191.
17. Lee, H.-G. (1999) *Chemical Thermodynamics for Metals and Materials*; Imperial College Press: London.
18. Trifunović, O.; Trägårdh, G. (2005) The influence of support layer on mass transport of homologous series of alcohols and esters through composite pervaporation membranes. *J. Membr. Sci.*, *259* (1–2): 122–134.
19. Pereira, C.C.; Ribeiro, C.P.J.; Nobrega, R.; Borges, C.P. (2006) Pervaporative recovery of volatile aroma compounds from fruit juices. *J. Membr. Sci.*, *274* (1–2): 1–23.
20. Pereira, C.C.; Habert, A.C.; Nobrega, R.; Borges, C.P. (1998) New insights in the removal of diluted volatile organic compounds from dilute aqueous solution by pervaporation process. *J. Membr. Sci.*, *138* (2): 227–235.
21. Trifunović, O.; Lipnizki, F.; Trägårdh, G. (2006) The influence of process parameters on aroma recovery by hydrophobic pervaporation. *Desalination*, *189*: 1–12.
22. Karlsson, H.O.E.; Trägårdh, G. (1994) Aroma compound recovery with pervaporation—the effect of high ethanol concentrations. *J. Membr. Sci.*, *91* (1–2): 189–198.
23. Feng, X.S.; Huang, R.Y.M. (1996) Estimation of activation energy for permeation in pervaporation processes. *J. Membr. Sci.*, *118* (1): 127–131.
24. Barrer, R.M. (1939) Activated diffusion in membranes. *Trans. Faraday Soc.*, *35*: 644–656.
25. Zheng, J.M.; Qiu, J.; Madeira, L.M.; Mendes, A. (2007) Polymer structure and the compensation effect of the diffusion pre-exponential factor and activation energy of a permeating solute. *J. Phys. Chem. B*, *111* (11): 2828–2835.
26. Yampolskii, Y.; Shishatskii, S.; Alentiev, A.; Loza, K. (1998) Correlations with and prediction of activation energies of gas permeation and diffusion in glassy polymers. *J. Membr. Sci.*, *148* (1): 59–69.
27. van Krevelen, D.W. (1990) *Properties of Polymers: Their Correlation with Chemical Structure; their Numerical Estimation and Prediction from Additive Group Contributions*, 3rd ed.; Elsevier: Amsterdam, The Netherlands.
28. Aminabhavi, T.M.; Phayde, H.T.S.; Ortego, J.D.; Vergnaud, J.M. (1996) Sorption/diffusion of aliphatic esters into tetrafluoroethylene/propylene

copolymeric membranes in the temperature interval from 25 to 70°C. *Eur. Polym. J.*, *32* (9): 1117–1126.
29. Pönitsch, M.; Kirchheim, R. (1996) Relation between prefactor and activation energy for the diffusion of atoms and small molecules in polymers. *Scripta Materialia*, *34* (9): 1479–1482.
30. Zener, C. (1951) Theory of D_0 for atomic diffusion in metals. *J. Appl. Phys.*, *22* (4): 372–375.
31. Liu, L.; Guo, Q.X. (2001) Isokinetic relationship, isoequilibrium relationship, and enthalpy-entropy compensation. *Chem. Rev.*, *101* (3): 673–695.
32. Kwei, T.K.; Arnheim, W. (1962) Linear free-energy relationship in the diffusion of gases through polymer films. *J. Chem. Phys.*, *37*: 1900–1901.
33. Barrer, R.M.; Skirrow, G. (1948) Transport and equilibrium phenomena in gas-elastomer systems. I. Kinetic phenomena. *J. Polym. Sci.*, *3* (4): 549–563.
34. Prabhakar, R.S.; Raharjo, R.; Toy, L.G.; Lin, H.Q.; Freeman, B.D. (2005) Self-consistent model of concentration and temperature dependence of permeability in rubbery polymers. *Ind. Eng. Chem. Res.*, *44* (5): 1547–1556.
35. Aguerre, R.J.; Suárez, C.; Viollaz, P.E. (1986) Enthalpy-entropy compensation in sorption phenomena: Application to the prediction of the effect of temperature on food isotherms. *J. Food Sci.*, *51* (6): 1547–1549.
36. Bell, R.P. (1937) Relations between the energy and entropy of solution and their significance. *Trans. Faraday Soc.*, *33*: 496–501.
37. Philibert, J. (2006) Some thoughts and/or questions about activation energy and pre-exponential factor. *Defect and Diffusion Forum*, *249*: 61–72.
38. Overington, A.; Wong, M.; Harrison, J.; Ferreira, L. (2008) Concentration of dairy flavour compounds using pervaporation. *Int. Dairy J.*, *18* (8): 835–848.
39. Borgnakke, C.; Sonntag, R.E. (1997) *Thermodynamic and Transport Properties*; John Wiley & Sons: New York.
40. Speight, J.G. (Ed.) (2003) *Perry's Standard Tables and Formulas for Chemical Engineers. Perry's Standard Tables and Formulas for Chemical Engineers*; McGraw-Hill: New York.
41. Lide, D.R. (Ed.) (2005) *CRC Handbook of Chemistry and Physics*; CRC Press: Boca Raton, Florida.
42. Poling, B.E.; Prausnitz, J.M.; O'Connell, J.P. (2001) *The Properties of Gases and Liquids*, 5th ed.; McGraw-Hill: New York.
43. Lipnizki, F.; Hausmanns, S. (2004) Hydrophobic pervaporation of binary and ternary solutions: Evaluation of fluxes, selectivities, and coupling effects. *Sep. Sci. Technol.*, *39* (10): 2235–2259.
44. Baudot, A.; Marin, M. (1999) Improved recovery of an ester flavor compound by pervaporation coupled with a flash condensation. *Ind. Eng. Chem. Res.*, *38* (11): 4458–4469.
45. Olsson, J.; Trägårdh, G. (1999) Influence of temperature on membrane permeability during pervaporative aroma recovery. *Sep. Sci. Technol. 34* (8): 1643–1659.
46. Carelli, A.A.; Crapiste, G.H.; Lozano, J.E. (1991) Activity coefficients of aroma compounds in model solutions simulating apple juice. *J. Agric. Food Chem.*, *39*: 1636–1640.

47. Börjesson, J.; Karlsson, H.O.E.; Trägårdh, G. (1996) Pervaporation of a model apple juice aroma solution: Comparison of membrane performance. *J. Membr. Sci.*, *119* (2): 229–239.
48. Dole, P.; Feigenbaum, A.E.; De la Cruz, C.; Pastorelli, S.; Paseiro, P.; Hankemeier, T.; Voulzatis, Y.; Aucejo, S.; Saillard, P.; Papaspyrides, C. (2006) Typical diffusion behaviour in packaging polymers—application to functional barriers. *Food Additives and Contaminants*, *23* (2): 202–211.
49. Tikhomirov, B.P.; Hopfenberg, H.B.; Stannett, V.; Williams, J.L. (1968) Permeation, diffusion, and solution of gases and water vapor in unplasticized poly(vinylchloride). *Die Makromolekulare Chemie*, *118*: 177–188.
50. Bicerano, J. (2002) *Prediction of Polymer Properties*, 3rd ed.; Marcel Dekker: New York.
51. Kabra, M.M.; Netke, S.A.; Sawant, S.B.; Joshi, J.B.; Pangarkar, V.G. (1995) Pervaporative separation of carboxylic acid-water mixtures. *Sep. Technol.*, *5* (4): 259–263.
52. Liang, L.; Ruckenstein, E. (1996) Pervaporation of ethanol-water mixtures through polydimethylsiloxane-polystyrene interpenetrating polymer network supported membranes. *J. Membr. Sci.*, *114* (2): 227–234.
53. Wang, P.; Guo, J.; Wunder, S.L. (1997) Surface stress of polydimethylsiloxane networks. *J. Polym. Sci. Pt. B-Polym. Phys.*, *35* (15): 2391–2396.
54. Shishatskii, A.M.; Yampolskii, Y.P.; Peinemann, K.V. (1996) Effects of film thickness on density and gas permeation parameters of glassy polymers. *J. Membr. Sci.*, *112* (2): 275–285.
55. Lötters, J.C.; Olthuis, W.; Veltink, P.H.; Bergveld, P. (1997) The mechanical properties of the rubber elastic polymer polydimethylsiloxane for sensor applications. *Journal of Micromechanics and Microengineering*, *7*: 145–147.
56. ten Hulscher, T.E.M.; Cornelissen, G. (1996) Effect of temperature on sorption equilibrium and sorption kinetics of organic micropollutants—a review. *Chemosphere*, *32* (4): 609–626.
57. Lamer, T.; Rohart, M.S.; Voilley, A.; Baussart, H. (1994) Influence of sorption and diffusion of aroma compounds in silicone rubber on their extraction by pervaporation. *J. Membr. Sci.*, *90*: 251–263.
58. Schäfer, T.; Heintz, A.; Crespo, J.G. (2005) Sorption of aroma compounds in poly(octylmethylsiloxane) (POMS). *J. Membr. Sci.*, *254* (1–2): 259–265.
59. Trifunović, O.; Trägårdh, G. (2003) The influence of permeant properties on the sorption step in hydrophobic pervaporation. *J. Membr. Sci.*, *216* (1–2): 207–216.
60. Djebbar, M.K.; Nguyen, Q.T.; Clément, R.; Germain, Y. (1998) Pervaporation of aqueous ester solutions through hydrophobic poly(ether-block-amide) copolymer membranes. *J. Membr. Sci.*, *146* (1): 125–133.
61. Kirchheim, R.; Huang, X.Y. (1987) A relationship between prefactor and activation energy for diffusion. *Phys. Status Solidi B-Basic Res.*, *144* (1): 253–257.
62. Budrugeac, P.; Segal, E. (1998) On the apparent compensation effect found for two parallel reactions. *Int. J. Chem. Kinet.*, *30* (9): 673–681.
63. Overington, A. (2008) *Concentration of dairy flavours using pervaporation.* PhD thesis (submitted), Massey University: Auckland, New Zealand.